GEOPHYSICAL RESEARCH LETTERS, VOL. 27, NO. 5, PAGES 601-604, MARCH 1, 2000

An empirical relationship between seismic attenuation and velocity anomalies in the upper mantle

[1]Erich G. Roth and Douglas A. Wiens

Department of Earth and Planetary Sciences, Washington University, Saint Louis, Missouri

Dapeng Zhao

Department of Earth Sciences, Ehime University, Matsuyama, JAPAN

Abstract. We use recent P wave attenuation (Q_α^{-1}) and velocity (V_p) tomographic models of the Tonga/Fiji region to obtain an empirical relation between attenuation and velocity for the upper mantle. The attenuation and velocity anomalies show a strong inverse correlation, allowing the determination of an empirical relationship. The relationship is similar to a predicted relation derived from laboratory experiments on peridotite and dunite, assuming the observed anomalies result from temperature variations. The results here suggest that the observed anomalies are generally consistent with the effect of temperature, and demonstrate that the combination of velocity and attenuation data provides powerful constraints on the physical state of upper mantle materials. We find that the chosen geotherm and activation energy has a strong effect on the position of the solidus within the seismic data.

Introduction

Many previous studies have observed that regions of slow seismic velocity are qualitatively correlated with zones of high seismic wave attenuation, suggesting that these anomalies are derived from similar thermal and tectonic processes [*Sheehan and Solomon*, 1992; *Romanowicz*, 1995]. Although this correlation has been apparent for some time, a quantitative comparison of Q (seismic quality factor which is inversely proportional to attenuation) and velocity has not been previously attempted. Regional attenuation models for areas with large absorption contrasts offer high resolution and large amplitude heterogeneity with which to approach this problem. Detailed models for the region surrounding the Tonga slab and Lau Basin have been generated using ocean bottom seismometer (OBS) and land broadband data in the Fiji Islands, Tonga Islands, and Niue Island. The area (Figure 1) is characterized by active backarc spreading, prolific deep seismicity, the world's fastest subduction rate [*Bevis et al.*, 1995], and large lateral variations in velocity and attenuation.

Attenuation and Velocity Models for the Tonga-Fiji Region

We use the attenuation model (Q_α) of [*Roth et al.*, 1999] for the region, derived from two different spectral decay methods in the frequency band 0.1 to 4.0 Hz. We express the attenuation anomaly, δQ^{-1}, for a particular block as the difference in Q_α^{-1} between the tomographic model and a global reference model, QM1 [*Widmer et al.*, 1991], such that positive values of δQ^{-1} indicate high attenuation. Figure 2a shows the percentage difference in $1/Q_\alpha$ between the local tomography and QM1. The use of other possible reference models, such as QR19 [*Durek and Ekstrom*, 1995] and QL6 [*Romanowicz*, 1995], produces little change in the results.

We compare the attenuation model to the P wave velocity tomography model of [*Zhao et al.*, 1997], with over 42,000 local and teleseismic arrivals. To compare the attenuation and velocity structures, the 3-D velocity model is converted to a 2-D model, and smoothed to simulate the lower resolution of the attenuation model. A velocity model is defined along the same trend as the 2-D attenuation model (Figure 1) by averaging velocities within a region extending 110 km on each side of the plane of projection. The velocity anomaly, δV_p, is defined as the difference between the P wave velocity in the tomographic model and the values in reference model IASP91 [*Kennett and Engdahl*, 1991], such that positive anomalies indicate fast velocities. Figure 2b shows the percentage difference in P wave velocity between the decimated tomography model and IASP91. Very little difference is observed between using IASP91 and PREM. The two tomography models show very similar features, including a steeply dipping slab extending down to at least 660 km depth and a high amplitude signature beneath the active back arc spreading center extending to at least 200 km.

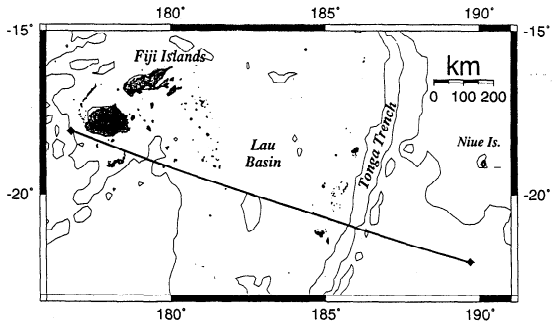

Figure 1. Map of the region showing the Tonga-Fiji region. The solid line indicates the projection of the two-dimensional attenuation tomography model on the surface, which approximately follows the main line of ocean bottom seismographs in the tomographic study. Contoured bathymetry is obtained from the National Geophysical Data Center.

[1]Now at U.S. Geological Survey, Woods Hole, Massachusetts

Paper number 1999GL005418.
0094-8276/00/1999GL005418$05.00

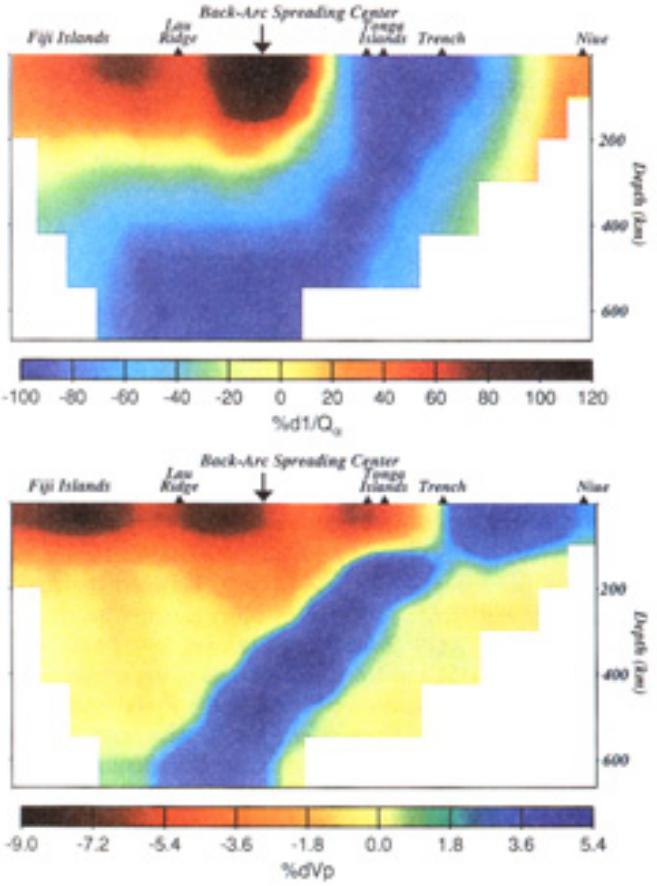

Figure 2. Cross sections projected along the line shown in Fig. 1, showing the percent difference between the tomographic models and global reference models. **a,** The Q_α model for the region, showing percent Q^{-1} anomaly relative to the global attenuation model QM1. High attenuation regions are shown in red and low attenuation regions are shown in blue. **b,** The *Vp* model for the region, showing velocity anomalies relative to the IASP91 velocity model. Major tectonic features are labeled along the top

Empirical Relationship Between Attenuation and Velocity.

We compare the attenuation and velocity models by plotting δQ^{-1} and δV_p against each other for the same spatial locations. As shown in Figure 3a, the velocity and attenuation anomalies beneath 100 km are strongly correlated, and the result is well fit by the empirical exponential equation,

$$\delta Q^{-1} = B + A_1 \exp(A_2 \bullet \delta V_p). \quad (1)$$

where A_1 = 0.0030 ± 0.0008 and A_2 = -4.83 ± 0.35, as determined by a least squares fit. The shallowest (0-100 km) data, although showing a general correlation, are rather scattered and are not included in the fitting procedure. A zero attenuation value at 100 km depth compared to a QM1 value of 200 gives a maximum negative attenuation anomaly of B = –0.005 [$(1/Q_{inf} - 1/200)$ = -0.005]. The observed inverse relationship is expected since hot regions will produce high values of δQ^{-1} and low values of δV_p. We also observe a depth effect, such that data from shallower depths have a high Q^{-1} anomaly and negative velocity anomaly, and the deeper data generally show lower Q^{-1} anomalies and higher δV_p.

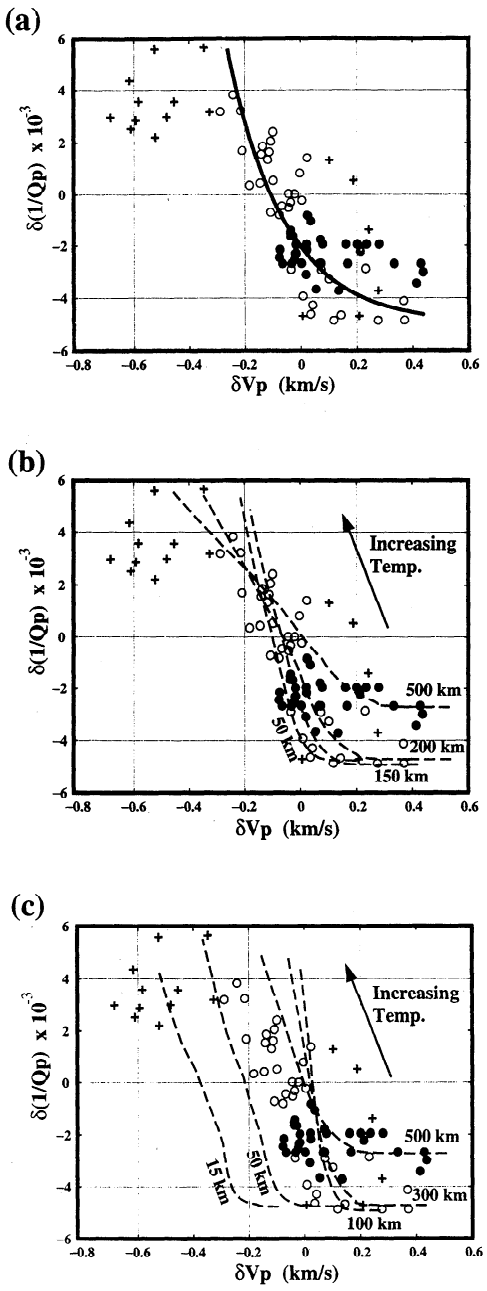

Figure 3. **a,** The relationship of velocity and attenuation anomalies for the models. Each point represents the Q^{-1} and V_p anomalies at one block in the attenuation model. Higher δQ^{-1} indicates lower values of Q_p in the tomography model, and higher δV_p indicates fast velocities. Crosses are used for data from depths of 0-100 km, open circles indicate data taken from 100-300 km and filled circles indicate data from 300-660 km. The solid curve represents the best exponential fit to the deeper (100-600 km) data set. In **b** and **c,** dashed curves represent the result of generating velocity and attenuation anomalies from experimental data, and are plotted with the observed seismic data for comparison. Each curve represents the effect of deviating from an oceanic geotherm at a particular depth, labeled on the figures. **b,** Attenuation anomalies are computed from the results of [*Sato et al.*, 1989a]. **c,** Shallow attenuation anomalies are computed from the results of [*Jackson et al.*, 1992] and are extrapolated to greater depth by scaling homologous Q with homologous temperature.

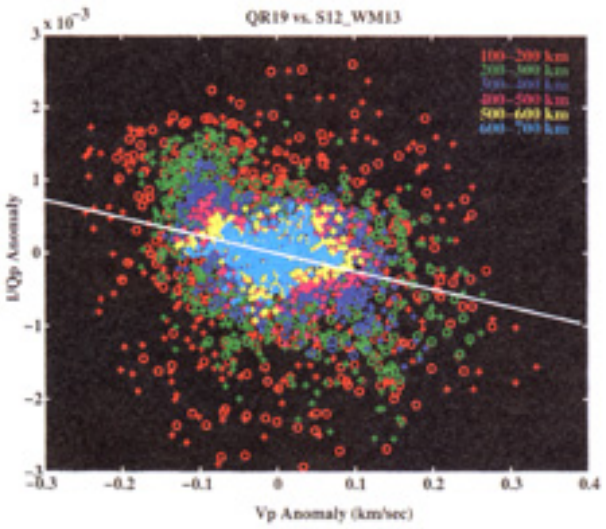

Figure 4. Results of plotting attenuation [*Romanowicz*, 1995] and velocity [*Su et al.*, 1994] anomalies relative to the QM1 and IASP91 1D reference earth models. Data is also binned into depth intervals to illustrate the lower overall range with increasing depth. The results of a least squares fit are also plotted.

This indicates that the average values of Q_α and V_p near the Tonga subduction zone are lower than global averages above 300 km, suggesting positive thermal anomalies, and higher at greater depths. Shallow depths are dominated by active back arc tectonics, mantle upwelling, and high heat flow, whereas at deeper areas, the rapid injection of cold slab material dominates the seismic structure.

The very large negative velocity anomalies at depths of less than 100 km lie off the trend of both the empirical fit to the deeper observations and most of the calculated relations. This may be due to the presence of melt beneath the Lau backarc spreading center. The presence of melt would produce much larger velocity reductions [*Sato and Sacks*, 1989] than would be expected from the simple temperature derivatives used in these calculations .

This approach is also attempted on a 3D global scale, using the velocity model S12_WM13 [*Su et al.*, 1994] and attenuation model QR19 [*Romanowicz*, 1995]. We have expanded QR19 to degree 6 and expressed it as a percentage difference from QM1 at 6 representative depths. We have also expanded S12_WM13 and expressed it as a percentage difference from IASP91 at the same depths. We plot the anomalies at evenly spaced points. The method of N. Sloane and R. Hardin of AT&T Bell Laboratories [*Peterson*, 1995] is used to generate the optimal arrangement of points on the globe with 6° of separation. As can be seen in Figure 4, these anomalies have a very weak correlation at best. The anomalies are also binned according to depth, with the individual "halos" corresponding to specific depth intervals. At shallower depths, the correlation between Q and V is slightly better than the fit to the dataset as a whole. It is also apparent that the shallower depths show the largest anomalies in both velocity and attenuation, a trend also seen in the Tonga-Fiji data. The possible explanation for this is that the global Q models do not yet have the resolution to distinguish strong lateral anelastic heterogeneity, but can resolve the variations in attenuation with depth. Improved global Q models will allow a more robust comparison to be made.

Comparison to Experimental Results.

It is often assumed that upper mantle anomalies result largely from lateral changes in temperature [*Forsyth*, 1975; *Anderson*, 1989]. We thus investigate whether the empirical relation we determine between δQ^{-1} and δV_p is compatible with the results of laboratory experiments, assuming that both the attenuation and velocity anomalies result from temperature anomalies. Throughout this study, we assume that the average mantle geotherm and solidus are given by [*Stacey*, 1977], and that this structure is compatible with global reference models. Velocity and attenuation anomalies are then caused by deviations from the *Stacey* [1977] geotherm. At a series of discrete depths, we evaluate a range of temperature anomalies and calculate the resulting velocity and attenuation anomaly. The calculated velocity anomalies are derived from the Q-dependent velocity derivatives, $\delta \ln V_p/\delta T$, of [*Karato*, 1993]. We also assume that the velocity anomaly is zero if the temperature anomaly relative to the global model (IASP91) is zero. The calculated velocity anomaly is expressed

$$\delta V_p = \exp\left[\left(\frac{\delta \ln V_p}{\delta T}\right)\delta T + \ln V_{IASPEI}\right] - V_{IASPEI} \qquad (2)$$

The value of the $\delta \ln V_p/\delta T$ used is determined from the Q predicted in laboratory results. The pressure variations come from the built in pressure dependence of Q along with the position of the mantle geotherm.

Comparison of seismic data with experimental data on peridotite

We show the results of using two different experimentally derived formulations for the relationship of attenuation and temperature. One set of laboratory studies on peridotite [*Sato et al.*, 1989; *Sato et al.*, 1989a] indicate that homologous Q, Q_H, is a function of homologous temperature, T_H, of the form,

$$Q_H = \exp[g(T_H - a)] \qquad (3)$$

where $Q_H = Q_\alpha/Q_{\alpha m}$, and $T_H = T_m/T$. $Q_{\alpha m}$ is Q_α at the melting temperature, T_m is the melting temperature, and g and a are empirical constants. The experimental data suggest that $Q_{\alpha m}$ is a linear function of pressure. The curves generated from these results show a very good fit to the seismic observables (Figure 3b). The strength of the *Sato* results is their ability to implicitly include the effects of depth. However, there does not seem to be a significant depth dependence for the experimental curves, which is consistent with our seismic observations for 100-660 km. However, the *Sato et al.* [1989, 1989a] relationships have been criticized for failing to account for the frequency dependence of attenuation.

Absorption band models for attenuation.

Another approach to estimating the temperature dependence of Q incorporates a series of experimental studies that fit the data using an absorption band model of attenuation [*Berkhemer et al.*, 1982; *Jackson et al.*, 1992; *Getting et al.*, 1997]. These studies model Q as a thermally activated process with a power law frequency dependence (ξ = 0.20-0.30), taking the form,

$$Q_\alpha^{-1}(T_o, T) = \gamma A[T_o \exp(-E^*/RT)]^\xi. \qquad (4)$$

Where T_o is oscillation period, T is temperature, R is the gas constant, ξE^* is the effective activation energy, and γ

represents the ratio of shear to compressional wave attenuation. In order to compare our P wave attenuation results with experimentally derived shear wave relations, we use the observed γ of 0.57 derived for Tonga [*Roth et al.*, 1999]. Experimental data using forsterite [*Berkhemer et al.*, 1982], dunite [*Jackson et al.*, 1992], and MgO [*Getting et al.*, 1997] have been modeled at near surface pressures and seismic frequencies.

The results of [*Jackson et al.*, 1992] were determined at pressures equivalent to 15 km depth, and must be extrapolated to the greater depths used in this study. We use a homologous Q scaling to do this extrapolation [*Sato and Sacks*, 1989; *Getting et al.*, 1997]. Q_α is first computed as a function of temperature for shallow (<15 km) depth using the *Jackson et al.* [1992] relationships. We then convert the Q_α values to homologous Q values ($Q_H = Q_\alpha/Q_{\alpha m}$), each of which is associated with a homologous temperature $T_H = T_m/T$. It is assumed that the same relationship between Q_H and T_H holds for deeper depths [*Getting et al.*, 1997]. $Q_{\alpha m}$ is readily calculated at greater depths, as $Q_{\alpha m}$ is observed to be a linear function of pressure [*Sato and Sacks*, 1989]. Since the Q_H - T_H relationship is known from the experiments, it is possible to estimate Q_α for a range of homologous temperatures at any depth. The values of Q_α are then converted to δQ^{-1}.

The results of this method of extrapolation are shown in Figure 3c along with the empirical data. Since the attenuation approaches zero at low temperatures, each curve asymptotes to the value of –1/QM1 for the sampled depth. The calculated curves for 15 and 50 km pass through most of the 0-100 km seismic data, which are rather scattered. The relative positions of consecutively deeper curves shift towards higher values of dV_p as the geotherm approaches the melting temperature. At greater depths (>100 km), the calculated curves are more closely spaced and match the region denoted by the 100-660 km seismic data. The good fit of the observed and calculated attenuation-velocity relationships lends support to the assumption that both attenuation and velocity variations arise primarily from thermal anomalies. The remaining discrepancies could be due to uncertainties in the effects of pressure, mineralogy, and temperature gradients.

Conclusions

This work shows that an empirical relation between attenuation and velocity anomalies can be derived and that it is consistent with experimental relationships between temperature and the seismic observables. The details of the calculated curves and the inferred mantle temperature anomalies depend on the global average geotherm and the mantle melting temperatures used, for which there is considerable uncertainty [*Hofmeister*, 1999]. We choose the *Stacey* [1977] values since they are widely cited in the literature and are internally consistent. Nonetheless, this study suggests that, with improved seismic models and laboratory data, important inferences about the thermal state of the earth's mantle can be made by combining velocity and attenuation data. Further progress is being made on fine-grained synthetic olivine aggregates and coarse-grained natural rocks that may strengthen the empirical relationship found here. Such experimental work will help better constrain effect of frequency, grain size, and composition on activation energy, attenuation, and velocity.

Acknowledgements. Equipment for the SPaSE deployment were obtained from the PASSCAL program of the Incorporated Research Institutions in Seismology (IRIS). This research was supported by the National Science Foundation under grants EAR9219675, OCE9314446, EAR9614502, and EAR9712311.

References

Anderson, D.L., *Theory of the Earth*, 366 pp., Blackwell Scientific Publications, Boston, 1989.

Berkhemer, H., W. Kampfman, E. Aulbach, and H. Schmeling, Shear modulus and Q of forsterite and dunite near partial melting from forced-oscillation experiments, *Phys. Earth Planet. Int.*, *29*, 30-41, 1982.

Bevis, M., F.W. Taylor, B.E. Schutz, J. Recy, B.L. Isacks, S. Helu, R. Singh, E. Kendrick, J. Stowell, B. Taylor, and S. Calmant, Geodetic observations of very rapid convergence and back-arc extension at the Tonga arc, *Nature*, *374*, 249-251, 1995.

Durek, J.J., and G.E. Ekstrom, Evidence of bulk attenuation in the asthenosphere from recordings of the Bolivia earthquake, *Geophys. Res. Lett.*, *22* (16), 2309-2312, 1995.

Forsyth, D.W., The early structural evolution and anisotropy of the oceanic upper mantle, *Geophys. J. Roy. astr. Soc.*, *43*, 103-162, 1975.

Getting, I.C., S.J. Dutton, P.C. Burnley, S. Karato, and H.A. Spetzler, Shear attenuation and dispersion in MgO, *Phys. Earth Planet. Int.*, *99*, 249-257, 1997.

Hofmeister, A.M., Mantle values of thermal conductivity and the geotherm from phonon lifetimes, *Science*, *283*, 1699-1706, 1999.

Jackson, I., M.S. Paterson, and J.D. Fitz Gerald, Seismic wave dispersion and attenuation in Aheim dunie: an experimental study, *Geophys. J. Int.*, *108*, 517-534, 1992.

Karato, S., Importance of anelasticity in the interpretation of seismic tomography, *Geophys. Res. Lett.*, *20*, 1623-1626, 1993.

Kennett, B.L.N., and E.R. Engdahl, Traveltimes for global earthquake location and phase identification, *Geophys J. Int.*, *105*, 429-465, 1991.

Peterson, I., The Codemart Catalog; Arranging points on a sphere for fun and profit, *Science News*, *147*, 140-141, 1995.

Romanowicz, B., A global tomographic model of shear attenuation in the upper mantle, *J. Geophys. Res.*, *100* (B7), 12,375-12,394, 1995.

Roth, E.G., D.A. Wiens, L. Dorman, J. Hildebrand, and S.C. Webb, Seismic attenuation tomography of the Tonga-Fiji region using phase pair methods, *J. Geophys. Res.*, *104*, 4795-4809, 1999.

Sato, H., and I.S. Sacks, Anelasticity and thermal structure of the oceanic upper mantle: Temperature calibration with heat flow data, *Journal of Geophysical Research*, *94*, 5705-5715, 1989.

Sato, H., S. Sacks, T. Murase, G. Muncill, and H. Fukuyama, Q_P-melting temperature relation in peridotite at high pressure and temperature: Attenuation mechanism and implications for the mechanical properties of the upper mantle, *Journal of Geophysical Research*, *94*, 10,647-10,661, 1989a.

Sheehan, A.F., and S.C. Solomon, Differential shear wave attenuation and its lateral variation in the North Atlantic region, *J. Geophys. Res.*, *97* (B11), 15,339-15,350, 1992.

Stacey, F.D., A thermal model of the Earth, *Phys. Earth Planet. Int.*, *15*, 341-348, 1977.

Su, W.-J., R.L. Woodward, and A.M. Dziewonski, Degree-12 model of shear velocity heterogeneity in the mantle, *J. Geophys. Res.*, *99*, 6945-6980, 1994.

Widmer, R., G. Masters, and F. Gilbert, Spherically symmetric attenuation within the Earth from normal mode data, *Geophys. J. Int.*, *104*, 541-553, 1991.

Zhao, D., Y. Xu, D.A. Wiens, L. Dorman, J. Hildebrand, and S. Webb, Depth extent of the Lau back-arc spreading center and its relationship to the subduction process, *Science*, 278, 254-257, 1997.

E. Roth and D. Wiens, Department of Earth and Planetary Sciences, Washington University, One Brookings Drive, St. Louis, Missouri, 63130 (e-mail: erich@izu.wustl.edu)

D. Zhao, Department of Earth Sciences, Ehime University, Matsuyama 790, JAPAN

(Received October 10, 1999; revised October 20, 1999; accepted Nov. 4, 1999)